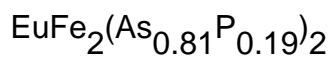


Correlation between intercalated magnetic layers and superconductivity in pressurized



This content has been downloaded from IOPscience. Please scroll down to see the full text.

2015 EPL 111 57007

(<http://iopscience.iop.org/0295-5075/111/5/57007>)

View [the table of contents for this issue](#), or go to the [journal homepage](#) for more

Download details:

IP Address: 162.105.145.52

This content was downloaded on 15/12/2015 at 06:17

Please note that [terms and conditions apply](#).

# Correlation between intercalated magnetic layers and superconductivity in pressurized $\text{EuFe}_2(\text{As}_{0.81}\text{P}_{0.19})_2$

JING GUO<sup>1,2</sup>, QI WU<sup>2</sup>, JI FENG<sup>1,6</sup>, GENFU CHEN<sup>2</sup>, TOMOKO KAGAYAMA<sup>3</sup>, CHAO ZHANG<sup>2</sup>, WEI YI<sup>2</sup>, YANCHUN LI<sup>4</sup>, XIAODONG LI<sup>4</sup>, JING LIU<sup>4</sup>, ZHENG JIANG<sup>5</sup>, XIANGJUN WEI<sup>5</sup>, YUYING HUANG<sup>5</sup>, KATSUYA SHIMIZHU<sup>3</sup>, LILING SUN<sup>2,6(a)</sup> and ZHONGXIAN ZHAO<sup>2,6(b)</sup>

<sup>1</sup> International Center for Quantum Materials, School of Physics, Peking University - Beijing 100871, China

<sup>2</sup> Institute of Physics and Beijing National Laboratory for Condensed Matter Physics, Chinese Academy of Sciences Beijing 100190, China

<sup>3</sup> KYOKUGEN, Graduate School of Engineering Science, Osaka University - Machikaneyama-cho 1-3, Toyonaka, Osaka 560-8531, Japan

<sup>4</sup> Institute of High Energy Physics, Chinese Academy of Sciences - Beijing 100039, China

<sup>5</sup> Shanghai Synchrotron Radiation Facilities, Shanghai Institute of Applied Physics, Chinese Academy of Sciences Shanghai 201204, China

<sup>6</sup> Collaborative Innovation Center of Quantum Matter - Beijing, 100190 and 100871, China

received 24 February 2015; accepted in final form 26 August 2015

published online 28 September 2015

PACS 74.70.Xa – Pnictides and chalcogenides

PACS 74.62.Fj – Effects of pressure

**Abstract** – We report comprehensive high-pressure studies on the correlation between intercalated magnetic layers and superconductivity in a  $\text{EuFe}_2(\text{As}_{0.81}\text{P}_{0.19})_2$  single crystal through *in situ* high-pressure resistance, specific-heat, X-ray diffraction and X-ray absorption measurements. We find that an unconfirmed magnetic order of the intercalated layers coexists with superconductivity in a narrow pressure range 0–0.5 GPa, and then it converts to a ferromagnetic (FM) order at pressure above 0.5 GPa, where its superconductivity is absent. The obtained temperature-pressure phase diagram clearly demonstrates that the unconfirmed magnetic order can emerge from the superconducting state. In stark contrast, the superconductivity cannot develop from the FM state that is evolved from the unconfirmed magnetic state. High-pressure X-ray absorption (XAS) measurements reveal that the pressure-induced enhancement of Eu's mean valence plays an important role in suppressing the superconductivity and tuning the transition from the unconfirmed magnetic state to a FM state. The unusual interplay among valence state of Eu ions, magnetism and superconductivity under pressure may shed new light on understanding the role of the intercalated magnetic layers in Fe-based superconductors.



Copyright © EPLA, 2015

A central issue in the studies of superconductivity has been the relationship between magnetism and superconductivity. For conventional superconductors, it is firmly believed that magnetism is hostile to superconductivity, as pointed out by Matthias rule [1]. While, for unconventional superconductors with layered structures constructed by conducting layers with magnetism and the intercalated layers without magnetism, such as cuprates or most of the iron pnictide superconductors, the emergence of superconductivity is closely connected with a

suppressed long-ranged antiferromagnetic (AFM) order of the conducting layers.  $\text{EuFe}_2\text{As}_2$  (Eu-122) and  $\text{CeFeAsO}$  are the peculiar members in Fe-based superconductors that contain dual AFM orders, one of which is from the FeAs layers as usual pnictide superconductors, and the other from the intercalated Eu or CeO layers [2–4]. Moreover, the Eu-122 compound was the only system with the feature of the intercalated layers with magnetism that can coexist with superconductivity in the high- $T_c$  superconductors, before the recent discovery of the  $\text{LiFeOHFeSe}$  superconductor [5]. For this kind of systems, what the role of the magnetism from the intercalated layers is in developing superconductivity is an intriguing issue.

(a) E-mail: llsun@iphy.ac.cn

(b) E-mail: zhxzha@iphy.ac.cn

At ambient pressure, the pristine Eu-122 is not superconducting (NSC), while phosphorous (P) doping can effectively suppress the AFM order of FeAs layers and induce a superconducting transition in the host sample, while tuning the AFM order of Eu ions to an alternative magnetic order. The type of the magnetic order of Eu ions that coexists with superconductivity is under debate. Some results show that this magnetic order state is a FM state [6–9], while others give evidence that it is an AFM state [10–12] or a canted AFM state plus spin glass [13]. Applying an external pressure plays a similar role as that of the chemical pressure induced by P doping, driving the undoped Eu-122 to a superconducting state (SC) for pressures ranging from 2.6 to 2.8 GPa and turning the magnetic state of the intercalated layers from the AFM to an unconfirmed magnetic state (UM) simultaneously [14–17]. In this study, we are the first to focus on the intercalated Eu layers in the  $\text{EuFe}_2(\text{As}_{0.81}\text{P}_{0.19})_2$  superconductor, and demonstrate the pressure-induced evolutions of the magnetic order from the intercalated layers, superconductivity, Eu’s valence state and lattice parameter in  $\text{EuFe}_2(\text{As}_{0.81}\text{P}_{0.19})_2$ . Our results reveal that the UM order can emerge from the superconducting state while the superconductivity cannot develop from the FM state. We propose that the UM-FM transition of the intercalated layers and the SC-NSC transition in pressurized  $\text{EuFe}_2(\text{As}_{0.81}\text{P}_{0.19})_2$  are associated with pressure-induced changes of the Eu’s valence state and lattice parameters.

The single crystals were synthesized by solid reaction methods, as described elsewhere [18]. The actual chemical composition for the host sample is inspected by inductive coupled plasma-atomic emission spectrometer, the resulting composition of which is  $\text{EuFe}_2(\text{As}_{0.81}\text{P}_{0.19})_2$ . High pressure is created by a diamond anvil cell (DAC). Diamond anvils of 600  $\mu\text{m}$  and 300  $\mu\text{m}$  flat tips were used for the low- and high-pressure measurements, respectively. Non-magnetic rhenium gaskets were used for different experimental runs. The  $\text{EuFe}_2(\text{As}_{0.81}\text{P}_{0.19})_2$  single crystal with dimensions around  $150 \times 120 \times 20 \mu\text{m}$  was loaded in the gasket hole and then confined in the hole by squeezing the two anvils. To achieve hydrostatic and quasi-hydrostatic pressure environments for the sample, silicon oil and NaCl powder were employed as pressure transmitting media for high-pressure specific-heat and resistance measurements, respectively. The details of high-pressure electrical resistance and ac-calorimetric measurements can be found in ref. [19] and ref. [20]. High-pressure angle-dispersive X-ray diffraction (XRD) and X-ray absorption spectra (XAS) measurements were carried out at the beamline 4W2 at Beijing Synchrotron Radiation Facility (BSRF) and at the beamline 14W at Shanghai Synchrotron Radiation Facility (SSRF), respectively. In the XRD measurements, a spring steel gasket with a hole about 120  $\mu\text{m}$  in diameter was used over the entire pressure range. The XAS measurements were performed with a side incidence, and a beryllium gasket with the same geometry was used in order to obtain a sufficient sample

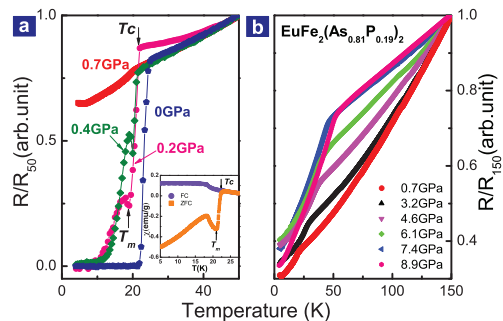


Fig. 1: (Colour on-line) Electrical resistance as a function of temperature for a  $\text{EuFe}_2(\text{As}_{0.81}\text{P}_{0.19})_2$  single crystal at different pressures. The inset displays dc magnetic susceptibility as a function of temperature, demonstrating the coexistence of superconductivity and the magnetic order.

signal. Silicon oil was employed as a pressure-transmitting medium to ensure the sample in a hydrostatic pressure environment in the XRD and XAS measurements. Pressure was determined by ruby fluorescence [21].

Figure 1 shows the temperature dependence of the electrical resistance of the  $\text{EuFe}_2(\text{As}_{0.81}\text{P}_{0.19})_2$  single crystal at different pressures. It can be seen that, at ambient pressure, the host sample shows a sharp resistance drop and presents the superconducting transition at a temperature ( $T_c$ ) of 24.5 K. Magnetic-susceptibility data measured at ambient pressure clearly exhibit the coexistence of the superconductivity and the magnetic order of Eu ions (inset of fig. 1(a)). By applying a pressure  $\sim 0.2$  GPa,  $T_c$  decreases apparently and the magnetic order of the intercalated layers becomes visible concomitantly at a temperature below  $T_c$  (fig. 1(a)). Here, we define the onset temperature of this magnetic order as  $T_m$ . Upon increasing pressure to 0.7 GPa, we find that the sample loses its zero resistance and the sharp transition becomes obliterated. Instead, a clear kink is present. Upon further increasing pressure, the resistance kink shifts to higher temperatures. At 8.9 GPa, the onset temperature of the resistance kink is about 48.3 K (fig. 1(b)). This resistance kink at pressure above 0.5 GPa has been confirmed by experiments to be a signature for the FM transition of the intercalated layers [15]. Here we define the onset temperature of the FM transition as  $T'_m$ .

Next, high-pressure ac-calorimetric and resistance measurements are performed. As shown in fig. 2, the measurements of electrical resistance as a function of temperature show two phase transitions at pressure below 0.5 GPa, one of which is related to the superconducting transition and the other to the PM-UM transition of the intercalated layers. It is a reproducible result that  $T_c$  decreases with increasing pressure and vanishes at 0.7 GPa (fig. 2(a)), and it is also consistent with our first run’s measurements (fig. 1(a)). Note that the transition of the PM-UM at  $T_m$  is more pronounced at 0.5 GPa, and, moreover, the resistance of the sample is enhanced around  $T_m$ . High-pressure specific-heat measurement is an effective

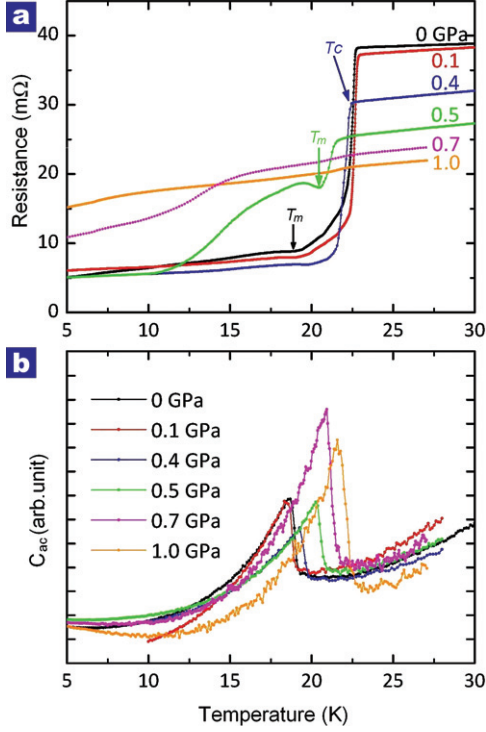


Fig. 2: (Colour on-line) Temperature dependence of (a) electrical resistance and (b) ac-calorimetric measurements of a  $\text{EuFe}_2(\text{As}_{0.81}\text{P}_{0.19})_2$  single crystal under pressure below 1 GPa.

way to identify the transition of magnetic orders. Figure 2(b) displays the plot of specific heat ( $C_{ac}$ ) vs. temperature at different pressures. We find a clear  $C_{ac}$  jump for the pressure-free sample, indicating the existence of the magnetic order in the host sample, in good agreement with our magnetic-susceptibility measurements (inset of fig. 1(a)). Upon increasing pressure, the  $C_{ac}$  jump shifts steadily to the higher-temperature side. Moreover, the intensity of the  $C_{ac}$  jump is found to grow remarkably at 0.7 and 1.0 GPa. Combining all these high-pressure resistance data, we believe that the kink seen on the temperature-resistance curves is associated with the magnetic transition of the intercalated Eu ions.

We summarize our experimental results in fig. 3. It is found that  $T_c$  shows a decrease with increasing pressure, while  $T_m$  displays an opposite behavior with pressure. These two temperatures ( $T_c$  and  $T_m$ ) intersect at  $\sim 0.5$  GPa. Our results demonstrate a clear process of strong competition between superconductivity and UM order in pressurized  $\text{EuFe}_2(\text{As}_{0.81}\text{P}_{0.19})_2$ . Further increasing pressure to about 0.52 GPa, the UM state turns to a FM state [15] (inset of fig. 3), and  $T'_m$  is found to increase continuously with pressure up to  $\sim 10$  GPa. The phase diagram clearly demonstrates that a magnetic order can emerge from the superconducting state, while the superconductivity cannot develop from the ferromagnetic state.

To understand the observed correlation between superconductivity and magnetic orders in a pressurized  $\text{EuFe}_2(\text{As}_{0.81}\text{P}_{0.19})_2$  sample, we performed high-pressure

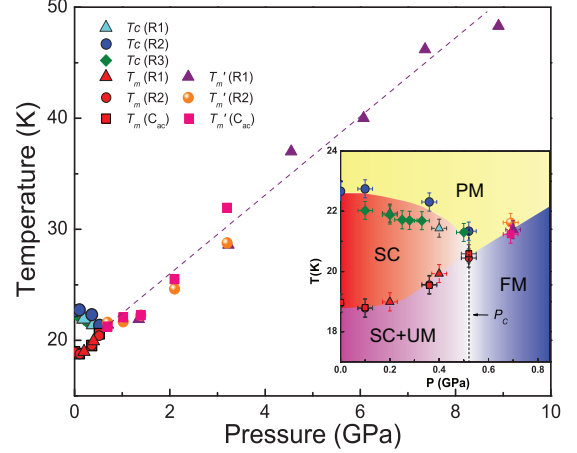


Fig. 3: (Colour on-line) Pressure-Temperature phase diagram of the  $\text{EuFe}_2(\text{As}_{0.81}\text{P}_{0.19})_2$  sample.  $T_c(R1)$ ,  $T_c(R2)$  and  $T_c(R3)$  stand for superconductivity transition temperatures obtained from different runs' resistance measurements,  $T_m(R1)$ ,  $T_m(R2)$  and  $T_m(C_{ac})$  represent the onset temperature of PM-UM transitions of the intercalated layers, which are determined from different runs' resistance and ac-calorimetric measurements, respectively.  $T'_m(R1)$ ,  $T'_m(R2)$  and  $T'_m(C_{ac})$  represent the onset temperature of PM-FM transitions, which are determined from different runs' resistance and ac-calorimetric measurements, respectively.  $T_c(R2)$  is obtained from the sample subjected to hydrostatic pressure, and  $T_c(R1)$  and  $T_c(R3)$  are obtained from the sample subjected to quasi-hydrostatic pressure.

XRD and XAS measurements in diamond anvil cells. No structural phase transition is found over the entire pressure range investigated (fig. 4(a)), suggesting that the pressure-induced disappearance of superconductivity is solely driven by the competition of the electron phases. Nevertheless, a remarkable reduction (compressed by 13.8% at  $\sim 9$  GPa) in the  $c$ -direction is observed. The pressure-induced shrinkage of the crystal lattice means a possible valence change of Eu ions because the volume of trivalent Eu with a  $4f^6$  electron shell is smaller than that of divalent Eu with a  $4f^7$  electron shell. To further study the basic connection among the valence change of Eu ions, superconductivity and magnetic state in  $\text{EuFe}_2(\text{As}_{0.81}\text{P}_{0.19})_2$ , we performed high-pressure XAS experiments on the Eu- $L_3$  absorption edge. As can be seen in the inset of fig. 4(b), the intensity of the main peak associated to the  $\text{Eu}^{2+}$  goes down, whereas the intensity of the satellite peak related to the  $\text{Eu}^{3+}$  goes up with increasing pressure. The spectra weight transfer indicates the occurrence of a valence change from  $\text{Eu}^{2+}$  to  $\text{Eu}^{3+}$ . We estimated the mean valence ( $\nu$ ) of Eu ions by the equation  $\nu = 2 + I^{\text{Eu}^{3+}} / (I^{\text{Eu}^{2+}} + I^{\text{Eu}^{3+}})$  [22,23], where  $I^{\text{Eu}^{2+}}$  and  $I^{\text{Eu}^{3+}}$  are the amplitudes of peaks corresponding to  $\text{Eu}^{2+}$  and  $\text{Eu}^{3+}$  on XAS spectrum, respectively. The estimated  $\nu$  of Eu ions in  $\text{EuFe}_2(\text{As}_{0.81}\text{P}_{0.19})_2$  single crystal was plotted in the main figure of fig. 4(b). Apparently,  $\nu$  is enhanced from 2.32 at ambient pressure up to 2.45 at 9.5 GPa. We also plot the pressure dependences of

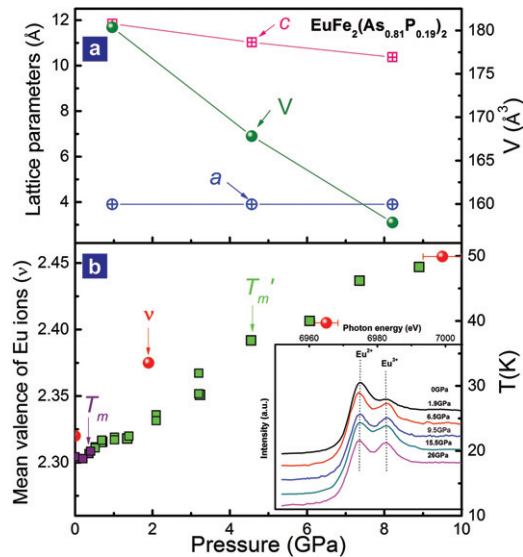


Fig. 4: (Colour on-line) (a) Pressure dependence of lattice parameters ( $a$  and  $c$ ), and unit cell volume ( $V$ ) in  $\text{EuFe}_2(\text{As}_{0.81}\text{P}_{0.19})_2$ . (b) Pressure dependences of mean valence ( $\nu$ ) of Eu ions, onset temperature ( $T_m$ ) of PM-UM transition and onset temperature ( $T'_m$ ) of PM-FM transition. The inset displays X-ray absorption spectra obtained at different pressures.

$T_m$  and  $T'_m$  in the same figure and find that the trends of pressure *vs.*  $\nu$ ,  $T_m$  and  $T'_m$  are the same, showing a monotonic increase with increasing pressure. Considering that P doping or external pressure can turn the magnetic order state of the intercalated layers from an AFM state to a UM state [6–10,15] where the valence of Eu ions changes from  $\text{Eu}^{2+}$  to  $\text{Eu}^{2.32+}$  at doping level of 0.38 and  $\text{Eu}^{2+}$  to  $\text{Eu}^{2.34+}$  at  $\sim 10$  GPa [15,18,24], we propose that the enhanced mean valence favors the AFM-UM-FM phase transitions. The pressure/doping-induced AFM-UM-FM transitions in the Eu-122 system are different from the case in  $\text{LiFeOHFeSe}$  [25], in which the AFM order state of the intercalated layers remains unchanged under chemical pressure due to the absence of such a kind of valence change of Eu ions as presented in the Eu-122 systems. From the dynamic point of view for the formations of superconducting and magnetic phases, our results indicate that the pressure-induced enhancement of the UM order state suppresses the superconductivity, and the FM order state, which is evolved from the UM order state when  $T_m$  is higher than  $T_c$ , definitely prevents the formation of the superconducting state. The enhancement of  $\nu$  is tightly related to the pressure-induced apparent reduction of the volume (fig. 4(a)).

In conclusion, the pressure-induced evolutions of the magnetic order in the intercalated layers, superconductivity, Eu's valence state and lattice parameter in  $\text{EuFe}_2(\text{As}_{0.81}\text{P}_{0.19})_2$  are clearly presented by comprehensive high-pressure studies. We find that, below 0.5 GPa,  $T_c$  decreases with increasing pressure, while  $T_m$  of the UM phase increases monotonically. At a critical pressure

$\sim 0.5$  GPa, superconductivity vanishes, and the UM state is switched to an FM state. Our results demonstrate that the UM state can emerge from the superconducting state and coexist with superconductivity, but the development of a superconducting state is prevented from the formation of a ferromagnetic state. Pressure-induced enhancement of the mean valence of Eu ions does not help to stabilize superconductivity but favors the UM-FM transition of the intercalated layers in  $\text{EuFe}_2(\text{As}_{0.81}\text{P}_{0.19})_2$ .

\*\*\*

The work was supported by the NSF of China (Grant Nos. 91321207 and 11427805), 973 projects (Grant Nos. 2011CBA00100 and 2010CB923000) and the Strategic Priority Research Program (B) of the Chinese Academy of Sciences (Grant No. XDB07020300).

## REFERENCES

- [1] PICKETT W. E., *Physica B*, **296** (2001) 112.
- [2] REN Z., ZHU Z. W., JIANG S., XU X. F., TAO Q., WANG C., FENG C. M., CAO G. H. and XU Z. A., *Phys. Rev. B*, **78** (2008) 052501.
- [3] XIAO Y., SU Y., MEVEN M., MITTAL R., KUMAR C. M. N., CHATTERJI T., PRICE S., PERSSON J., KUMAR N., DHAR S. K., THAMIZHAVEL A. and BRUECKEL TH., *Phys. Rev. B*, **80** (2009) 174424.
- [4] ZHAO J., HUANG Q., CRUZ C. D. L., LI S. L., LYNN J. W., CHEN Y., GREEN M. A., CHEN G. F., LI G., LI Z., LUO J. L., WANG N. L. and DAI P. C., *Nat. Mater.*, **7** (2008) 953.
- [5] LU X. F., WANG N. Z., WU H., WU Y. P., ZHAO D., ZENG X. Z., LUO X. G., WU T., BAO W., ZHANG G. H., HUANG F. Q., HUANG Q. Z. and CHEN X. H., *Nat. Mater.*, **14** (2014) 325.
- [6] REN Z., TAO Q., JIANG S., FENG C. M., WANG C., DAI J. H., CAO G. H. and XU Z. A., *Phys. Rev. Lett.*, **102** (2009) 137002.
- [7] NOWIK I., FELNER I., REN Z., CAO G. H. and XU Z. A., *J. Phys.: Condens. Matter*, **23** (2011) 065701.
- [8] CAO G. H., XU S. G., REN Z., JIANG S., FENG C. M. and XU Z. A., *J. Phys.: Condens. Matter*, **23** (2011) 464204.
- [9] AHMED A., ITOU M., XU S. G., XU Z. A., CAO G. H., SAKURAI Y., PENNER-HAHN J. and DEB A., *Phys. Rev. Lett.*, **105** (2010) 207003.
- [10] ZAPF S., WU D., BOGANI L., JEEVAN H. S., GEGENWART P. and DRESSEL M., *Phys. Rev. B*, **84** (2011) 140503(R).
- [11] TOKIWA Y., HÜBNER S.-H., BECK O., JEEVAN H. S. and GEGENWART P., *Phys. Rev. B*, **86** (2012) 220505(R).
- [12] MUNEVAR J., MICKLITZ H., ALZAMORA M., ARGÜELLO C., GOKO T., NING F. L., MUNSIE T., WILLIAMS T. J., ACZEL A. A., LUKE G. M., CHEN G. F., YU W., UEMURA Y. J. and BAGGIO-SAITOVITCH E., *Solid State Commun.*, **187** (2014) 18.
- [13] ZAPF S., JEEVAN H. S., IVEK T., PFISTER F., KLINGERT F., JIANG S., WU D., GEGENWART P., KREMER R. K. and DRESSEL M., *Phys. Rev. Lett.*, **110** (2013) 237002.

- [14] KURITA N., KIMATA M., KODAMA K., HARADA A., TOMITA M., SUZUKI H. S., MATSUMOTO T., MURATA K., UJI S. and TERASHIMA T., *Phys. Rev. B*, **83** (2011) 214513.
- [15] MATSUBAYASHI K., MUNAKATA K., ISOBE M., KATAYAMA N., OHGUSHI K., UEDA Y., KAWAMURA N., MIZUMAKI M., ISHIMATSU N., HEDO M., UMEHARA I. and UWATOKO Y., *Phys. Rev. B*, **84** (2011) 024502.
- [16] TERASHIMA T., KIMATA M., SATSUKAWA H., HARADA A., HAZAMA K., UJI S., SUZUKI H. S., MATSUMOTO T. and MURATA K., *J. Phys. Soc. Jpn.*, **78** (2009) 083701.
- [17] MICLEA C. F., NICKLAS M., JEEVAN H. S., KASINATHAN D., HOSSAIN Z., ROSNER H., GEGENWART P., GEIBEL C. and STEGLICH F., *Phys. Rev. B*, **79** (2009) 212509.
- [18] SUN L. L., GUO J., CHEN G. F., CHEN X. H., DONG X. L., LU W., ZHANG C., JIANG Z., ZOU Y., ZHANG S., HUANG Y. Y., WU Q., DAI X., LI Y. C., LIU J. and ZHAO Z. X., *Phys. Rev. B*, **82** (2010) 134509.
- [19] SUN L. L., CHEN X. J., GUO J., GAO P. W., HUANG Q. Z., WANG H. D., FANG M. H., CHEN X. L., CHEN G. F., WU Q., ZHANG C., GU D. C., DONG X. L., WANG L., YANG K., LI A. G., DAI X., MAO H. K. and ZHAO Z. X., *Nature*, **483** (2012) 67.
- [20] HOLMES A. T., JACCARD D. and MIYAKE K., *Phys. Rev. B*, **69** (2004) 024508.
- [21] MAO H. K., XU J. and BELL P. M., *J. Geophys. Res.*, **91** (1986) 4673.
- [22] DALLERA C., GRIONI M., PALENZONA A., TAGUCHI M., ANNESE E., GHIRINGHELLI G., TAGLIAFERRI A., BROOKES N. B., NEISIUS TH. and BRAICOVICH L., *Phys. Rev. B*, **70** (2004) 085112.
- [23] GRAZIOLI C., HU Z., KNUPFER M., GRAW G., BEHR G., GOLDEN M. S., FINK J., GIEFERS H., WORTMANN G. and ATTENKOFER K., *Phys. Rev. B*, **63** (2001) 115107.
- [24] KUMAR R. S., ZHANG Y., THAMIZHAVEL A., SVANE A., VAITHEESWARAN G., KANCHANA V., XIAO Y. M., CHOW P., CHEN C. F. and ZHAO Y. S., *Appl. Phys. Lett.*, **104** (2014) 042601.
- [25] LU X. F., WANG N. Z., LUO X. G., ZHANG G. H., GONG X. L., HUANG F. Q. and CHEN X. H., *Phys. Rev. B*, **90** (2014) 214520.